[2] R. Chadha and K. C. Gupta, "Segmentation method using impedance matrices for the analysis of planar microwave circuits," *IEEE Trans. Microwave Theory Tech.*, vol. MTT-29, pp. 71–74, Jan. 1981.
[3] T. Okoshi and T. Miyoshi, "The planar circuit—An approach to microwave integrated circuitry," *IEEE Trans. Microwave Theory Tech.*, vol. MTT-20, pp. 245–252, Apr. 1972.
[4] K. C. Gupta, R. Garg, and R. Chadha, *Computer Aided Design of Microwave Circuits*. Dedham, MA: Artech House, 1981, chs. 8 and 11.
[5] R. Mehran, "Calculation of microstrip bends and *Y*-junctions with arbitrary angle," *IEEE Trans. Microwave Theory Tech.*, vol. MTT-26, pp. 400–405, June 1978.
[6] G. Kompa, "*S*-matrix computation of microstrip discontinuities with a planar waveguide model," *Arch. Elek. Ubertragung.*, vol. 30, pp. 58–64, 1976.
[7] S. Ramo, J. R. Whinnery, and T. Van Duzer, *Fields and Waves in Communication Electronics*. New York: Wiley, 1965, p. 421.

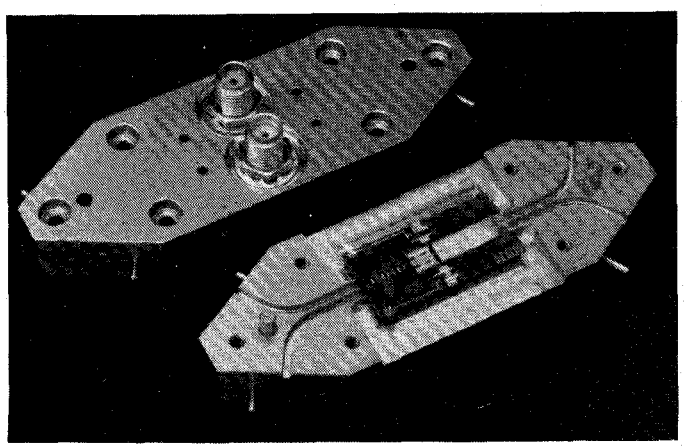

Fig. 1. *E*-plane balanced mixer.

E-Plane *W*-Band Printed-Circuit Balanced Mixer

PAUL J. MEIER, SENIOR MEMBER, IEEE

***Abstract*—A balanced *W*-band mixer has been developed which integrates a low-loss printed-probe hybrid with fin-line diode mounts on a single substrate. This *E*-plane approach features production economy, effective shielding, high (> 400) unloaded *Q*, light dielectric loading, and simple waveguide interfaces. With the LO fixed at 95 GHz, the measured conversion loss of the mixer is 7.8 ± 0.7 dB across the RF band of 92–98 GHz.**

I. Introduction

Continuing interest in the 3-mm atmospheric window has underscored the need for low-cost high-performance receivers. Balanced mixers are of special interest in radiometers where the IF is generally low, or in those applications where LO radiation must be minimized. A key component of a balanced mixer is the hybrid coupler which can be constructed in various forms. At millimeter wavelengths, the most common forms of printed-circuit hybrids have been the ring hybrid [1], the branch-line coupler [2], and the slot/coplanar/microstrip junction [3], [4]. Although existing designs can be scaled into the 3-mm band, problems are to be expected in terms of radiation, stray coupling, *Q* limitations, manufacturing tolerances, and interaction of waveguide transitions.

The printed-probe *E*-plane coupler has been developed [5], [6] as an alternative to the older forms of IC hybrids. A balanced mixer can be constructed entirely from *E*-plane lines [7] by integrating such a hybrid with fin-line diode mounts. Advantages of the *E*-plane approach at millimeter wavelengths include printed-circuit economy, negligible radiation and stray coupling, high unloaded *Q* (> 400 at 94 GHz), low-equivalent dielectric constant (for eased tolerances), and simple wide-band transitions to standard waveguide instrumentation.

This presentation reviews earlier component work [6], [7] that has not yet appeared in journal format, and describes the integration and performance of the balanced *E*-plane mixer.

II. Mixer Construction

Fig. 1 shows the *E*-plane *W*-band balanced mixer assembly. The major components, a seven-probe hybrid and a pair of fin-line diode mounts, are printed on a single board which is suspended in the *E*-plane of a four-port housing. All four ports were required in early tests of the hybrid alone. In the illustrated assembly only the two waveguide ports at the left are utilized. These ports serve as the RF and LO inputs. The IF outputs leave the housing through SMA connectors and are combined in a coax tee (not shown).

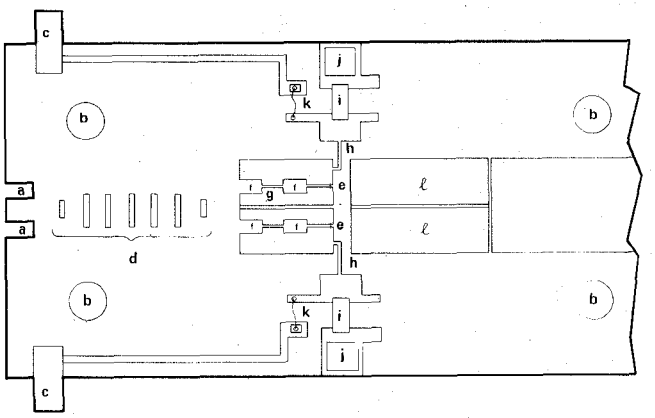

Fig. 2. Balanced mixer components.

Fig. 2 identifies the components of the printed-circuit assembly. Included are: a) quarter-wave notches which provide a match between the air-filled and slab-loaded waveguides, b) mounting holes which align the 5-mil, Duroid-5880 board within the housing, c) foil tabs where dc bias can be applied, d) seven-element printed-probe coupler, e) fin-line mounts for the beam-lead diodes, the mounts include f) RF transformers, g) gold wire that provides the ground return for the RF, LO, IF, and dc bias, h) IF output, containing high-impedance lines i) dc-blocking capacitors, j) connector contacts, k) resistors which block the IF from the dc bias circuit, and l) printed-circuit *E*-plane bifurcations which reactively terminate the diode mounts at RF and LO.

III. Printed-Probe Hybrid

At the center of the housing, shown in Fig. 1, parallel waveguides share a common broadwall. To accept a pair of dielectric boards, this broadwall is slotted. An array of coupling probes is printed on one board and insulated from the common wall by a second board that is fabricated from 2-mil Teflon.

The *E*-plane coupler was designed with the aid of the equivalent circuits shown in Fig. 3. The full circuit for a multielement coupler Fig. 3(a) can be reduced to the circuit of Fig. 3(b) for the modeling of isolated probes. The full circuit includes: a) genera-

Manuscript received March 16, 1982; revised May 26, 1982. This work was supported by Eaton Corporation's AIL Division.
The author is with the Eaton Corporation, AIL Division, Melville, NY 11747.

0018-9480/83/0200-0227$01.00 ©1983 IEEE

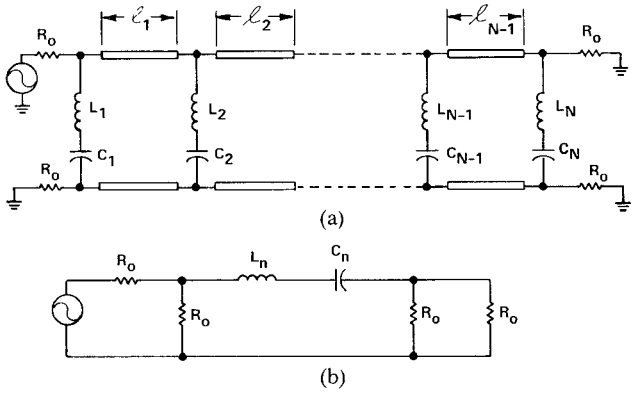

Fig. 3. Equivalent circuits. (a) N-element array. (b) Single element.

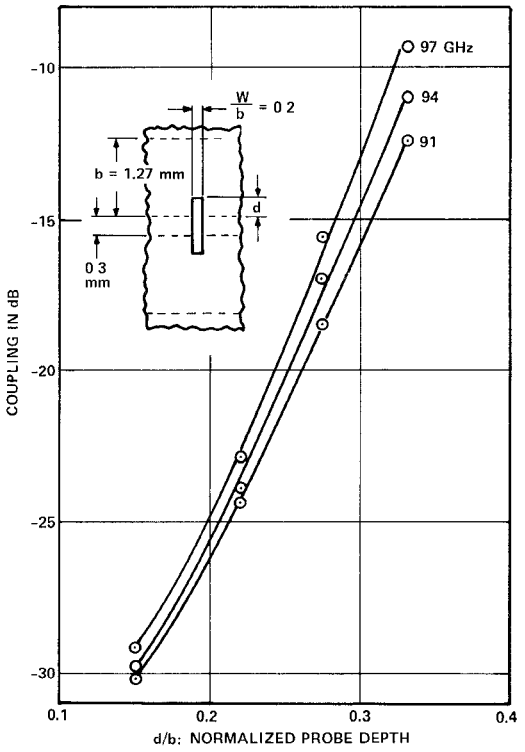

Fig 4 Coupling versus probe depth.

tor and load impedance R_0 whose value at each frequency of interest was calculated from the power-voltage definition, b) series LC branches which model the probe coupling elements, and c) lengths of slab-loaded waveguides, each with a characteristic impedance of R_0. R_0 may be calculated from

$$R_0 = \frac{754b}{a\sqrt{k_e - (\lambda/2a)^2}} \tag{1}$$

where a and b are the major and minor inner waveguide dimensions, k_e is the equivalent dielectric constant of the slab-loaded waveguide, and λ is the free-space wavelength. From a previous publication [8], it is known that k_e is 1.2 for the geometry under consideration.

The coupling elements were modeled by a computer-aided technique that determined the L and C values and provided the best fit with measurements. The modeling began with measurements of the coupling provided for by a series of boards each containing a single probe. Basic design information was obtained by measuring the coupling versus frequency for probes of various lengths and widths. After initial work with the probe width fixed at 4 mils, the width was increased to 10 mils for the final coupler

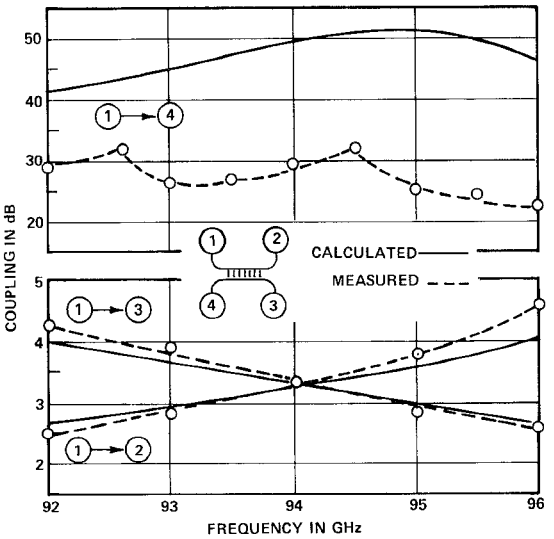

Fig. 5. Performance of seven-probe hybrid.

design. The increased width results in a lower parasitic series inductance, thereby decreasing the coupling variation across a given band. Also, increased width provides better reproducibility by minimizing the effect of undercutting.

Fig. 4 shows how the coupling of a 10-mil probe varies as a function of the depth that either end protrudes into a WR-10 waveguide. Across the 6-percent measurement band, the coupling varies ± 0.5 dB for a loosely coupled element ($d/b = 0.15$), but the variation is three times greater for a tightly coupled element ($d/b = 0.33$).

After studying a variety of array configurations, a seven-probe, equal-element coupler was chosen for the final design. The configuration is simple and compact. It avoids the large range in coupling levels found in more complex distributions (such as Chebychev). The preferred equal-element design avoids both tightly coupled elements (which have bandwidth limitations) and extremely loosely coupled elements (which contribute little to the overall 3-dB level).

The required midband coupling levels were determined for a 3-dB, seven-probe, equal-element array. Based on Fig. 4, the coupling/frequency characteristic for each element in the array was known and unique LC combinations were found (by a computer-aided analysis of Fig. 3(b) that correctly modeled the measurement. The results are as follows:

Element No.	Midband Coupling (dB)	L (nH)	C (fF)
1 and 7	−24.1	4.97	0.271
2–6	−18.1	5.55	0.345

The performance of the full array was calculated from the equivalent circuit in Fig. 3(a). All line lengths were initially set at a quarter-wavelength and then optimized by a gradient-search technique. After the circuit had been optimized, a prototype model was constructed and tested.

Fig. 5 shows the measured and calculated performance of the seven-probe coupler. Across a 3.7-GHz band, centered at 94 GHz, the measured isolation is 22 dB or better and the coupling to either output port is 3.4 ± 0.9 dB. In comparing the measurements with calculations, it should be noted that the measured isolation includes the effects of waveguide bends, flange discontinuities, and detector mismatch, whereas the model assumes perfect terminations.

At midband, the coupling is only 0.4 dB below the ideal 3-dB value. Since the housing alone has an insertion loss of 0.3 dB, the hybrid contributes only 0.1 dB to the total loss. Based on an axial length of 1.5 wavelengths, the unloaded Q in the printed probe region is greater than 400.

IV. Diode Mounts

Other important parts of the assembly depicted in Fig. 2 are the GaAs beam-lead mixer diodes, and the fin-line circuit in which they are mounted. The diodes chosen for this program were developed by Calviello *et al.* [9], [10] and have the following characteristics:

Zero-bias junction capacitance	5 fF
Package capacitance	20 fF
Series resistance	3 Ω
Ideality factor	1.07

The initial dimensions for the fin-line mounts were scaled from a related design [4]. The circuit was then optimized as a single-ended mount (that is, without the E-plane hybrid). Through observation of the reflected power with a waveguide coupler, the circuit was adjusted to be matched (across the band of interest) under typical bias conditions [7].

V. Mixer Integration and Performance

After optimizing the hybrid and diode mounts, these components were integrated to form the balanced mixer as shown in Fig. 1. Measurements of return loss, RF/LO isolation, and conversion loss were then performed.

Fig. 6 shows the measured return loss at the RF port of the balanced mixer under typical LO-drive conditions. With 6 dBm of LO power at 96 GHz, and a dc bias of 8 mA per diode, the return loss is 12 dB or better across the RF band of 93–98 GHz. Similar results were obtained by interchanging the RF and LO ports. The measured RF/LO isolation was 20 dB or better for typical drive conditions in the LO band of 94–96 GHz.

The conversion loss of the balanced mixer was measured for a wide range of RF and LO combinations. The RF power level was determined with a wide-band thermistor whose calibration was verified with a wet calorimeter. Fig. 7 shows the measured conversion loss versus the signal frequency with the LO frequency as a parameter. For these tests, the bias was fixed at 6 mA per diode and the power input to the LO port was 10 dBm. With the LO at 95 GHz, the measured conversion loss was 7.8 ± 0.7 dB across the RF band of 92–98 GHz. As shown, similar performance was obtained with the LO at 94 or 96 GHz.

Fig. 8 shows the measured conversion loss versus LO power with the dc bias as a parameter. In these tests, the LO and RF frequencies were 94.0 and 95.5 GHz, respectively. Although the minimum conversion loss is obtained with 6 mA and an LO power of 10 dBm, the variation in conversion loss with respect to LO power can be minimized by choosing a smaller bias current. With the bias fixed at 4 mA per diode, the measured conversion loss is 7.7 ± 0.1 dB for LO power levels of 4–10 dBm. By accepting a 1-dB degradation in the conversion loss, the LO power may be reduced to 0 dBm with the dc bias fixed at 2 mA.

Since the diodes have an excess noise ratio near unity [10], the double-sideband (DSB) noise figure of the mixer should be 3 dB lower than the conversion loss. To confirm this, the DSB noise figure was measured by switching hot (395 K) and cold (77 K) loads at the RF port, and observing the Y-factor at the IF port. As expected, the measured DSB noise figure was typically 6.3 dB, including a 1.5-dB contribution from a 30-MHz IF amplifier.

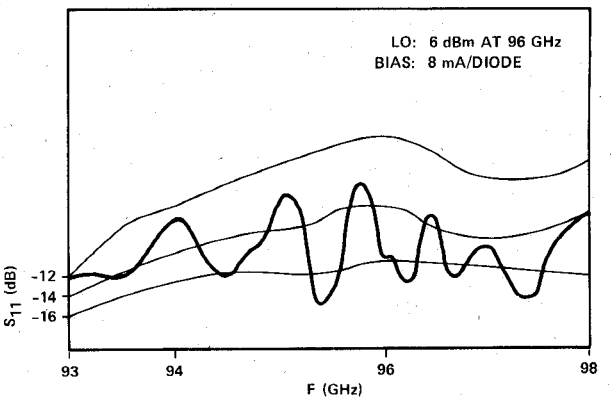

Fig. 6. Return loss at RF port.

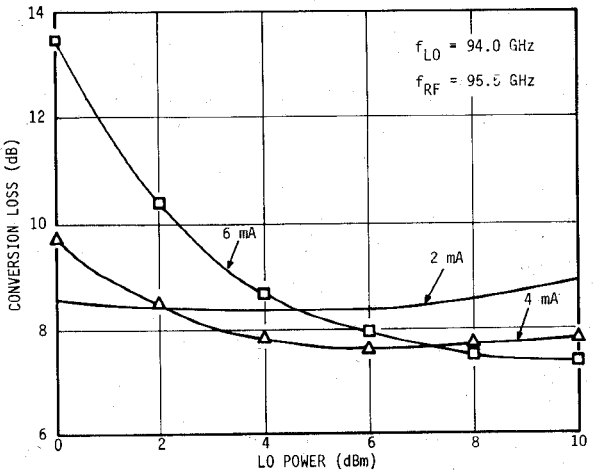

Fig. 7. Conversion loss of E-plane mixer.

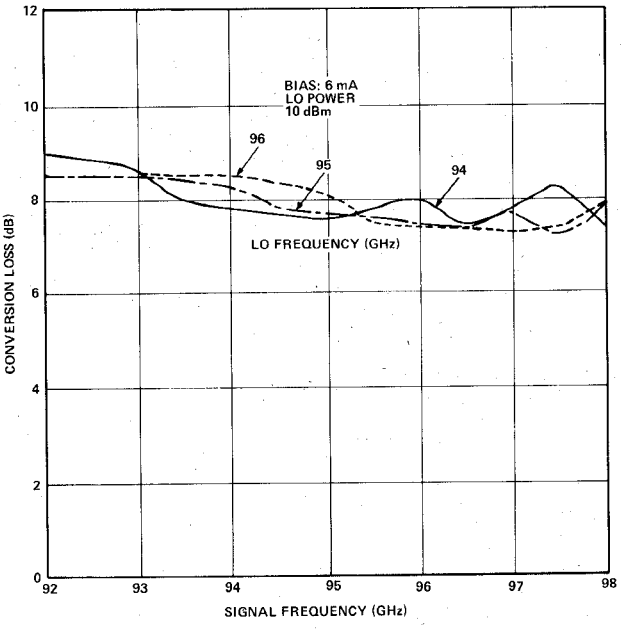

Fig. 8. Balanced mixer conversion loss versus LO power.

VI. Conclusion

A new form of a printed-circuit W-band balanced mixer has been designed, fabricated, and tested. This mixer, which integrated a printed-probe hybrid coupler and fin-line diode mounts, has a conversion loss of 7.8 ± 0.7 dB across a 6-GHz band

centered at 95 GHz. The bandwidth may be increased, if necessary, by adding probes to the hybrid [6], or by substituting another type of E-plane hybrid [11]. The housing utilized in this demonstration model can be greatly simplified by eliminating three of the four waveguide bends. (Two bends were used only in characterizing the hybrid, and a third bend could be replaced by a straight housing section.)

The E-plane approach provides advantages in terms of printed-circuit economy, effective shielding, high unloaded $Q(>400$ at 94 GHz), low equivalent dielectric constant (for eased production tolerances), and simple transitions to standard waveguide. The E-plane mixer is applicable to a wide range of advanced millimeter-wave systems including radars, communication links, and radiometers.

ACKNOWLEDGMENT

The work reported was sponsored by Eaton Corporations AIL Division, under the direction of M. Lebenbaum, B. Peyton, and J. Whelehan. The diodes were developed by J. Calviello and P. Bie of AIL's Central Research Laboratory under the direction of J. Taub. Technical assistance was provided by A. Cooley, A. Kunze, J. Pieper, A. Rees, and C. Thompson all of the AIL Division.

REFERENCES

[1] T H Oxley *et al*, "Hybrid microwave integrated circuits for millimeter wavelengths," in *Dig 1972 MTT Symp.*, May 1972, pp 224–226.
[2] T Araki and M Hirayama, "A 20-GHz integrated balanced mixer," *IEEE Trans Microwave Theory Tech*, vol. MTT-19, pp 638–643, July 1971.
[3] A K. Gorwara *et al*, "*K*-band image-reject and *Ka*-band balanced mixers constructed using planar millimeter-wave techniques," SRI Final Rep, Contract N00123-74-C-1957, Mar. 1975
[4] P J Meier, "Printed-circuit balanced mixer for the 4- and 5-mm bands," in *Dig. 1979 MTT Symp.*, Apr. 1979, pp. 84–86
[5] P J Meier, "Millimeter integrated circuits suspended in the E-plane of rectangular waveguide," *IEEE Trans Microwave Theory Tech.*, vol MTT-26, pp 726–773, Oct 1978.
[6] P. J. Meier, "Printed-probe hybrid coupler for the 3-mm band," in *Proc. 9th Eur Microwave Conf*, Sept 1979, pp 443–447
[7] P. J. Meier, "E-plane components for a 94-GHz printed-circuit balanced mixer," in *Dig 1980 MTT Symp.*, May 1980, pp. 267–269.
[8] P. H Vartanian *et al*, "Propagation in dielectric slab-loaded rectangular waveguide," *IRE Trans. Microwave Theory Tech.*, vol MTT-6, pp 215–222, Apr 1958
[9] J. A. Calviello, J. L Wallace, and P. R Bie, "High-performance GaAs beam-lead mixer diodes for millimeter and submillimeter applications," *Electron Lett*, vol 15, no 17, pp. 509–510, Aug 1979
[10] J A Calviello, S. Nussbaum, and P R Bie, "High-performance GaAs beam-lead mixer diodes for millimeter and submillimeter applications," in *Dig IEEE Int Electron Devices Meeting*, Dec 1981, pp 692–695
[11] E Kpodzo, K Schunemann, and G. Begemann, "A quadriphase fin-line modulator," *IEEE Trans. Microwave Theory Tech.*, vol. MTT-28, pp. 747–752, July 1980.

A Cryogenic Millimeter-Wave Schottky-Diode Mixer

ERIK L. KOLLBERG, MEMBER, IEEE,
AND HERBERT H. G. ZIRATH

***Abstract*—We report theoretical calculations and measurements on cryogenic millimeter-wave Schottky-diode mixers. Measurements of the embedding impedances at the signal and image frequencies have been used for the theoretical predictions of the mixer performance, and an excellent agreement with measured performance was obtained. Measurements of embedding impedances for various waveguide structures are reported, and the choice of configuration for optimum single-sideband performance is discussed.**

Manuscript received May 5, 1982; revised July 28, 1982. This work was supported (in part) by the Swedish Board for Technical Development

The authors are with the Department of Electron Physics I and Onsala Space Observatory, Chalmers University of Technology, Göteborg, Sweden

I. INTRODUCTION

Cooled millimeter-wave Schottky-diode mixers are frequently used in low-noise radiometer systems [1]–[4]. Although the superconducting semiconductor–insulator–semiconductor (SIS) mixer has still lower noise [5], it needs cooling to 4.2 K or below, while there is no use cooling the diode mixer below about 20 K [6]. Therefore, for most practical purposes, cooled diode mixers are at present the best choice for low-noise receivers. Below, we will report on some results obtained when developing the mixer receivers now in use at Onsala Space Observatory.

II. MIXER DESIGN

The mixers used are designed in a straightforward way (Fig. 1). An impedance transformer at the IF-output port matches the 50-Ω IF amplifier to the diode when dc-biased to have a differential dc-resistance $r = (di/dv)^{-1}$ equal to 175 Ω. This impedance level has been found to be a good compromise yielding a low-power reflection (less than about 1–2 dB extra conversion loss) for most bias conditions and the backshort settings where low-noise operations are obtained. The diode is mounted in a reduced-height waveguide in order to facilitate impedance matching. In Fig. 2, a typical locus of the diode impedance (the complex conjugate) versus dc- and local-oscillator bias is shown. The waveguide cross-section dimensions, the length and the shape of the whisker, the low-pass filter impedance, and the position of the diode chip in the waveguide are the most important parameters that influence the locus of the impedance circle, representing the embedding impedance seen by the diode, obtained when the backshort (l_b) is moved over $\lambda_g/2$ (see Fig. 2).

In Fig. 3, an equivalent embedding circuit is shown. The inductive (X_L) and capacitive (X_{C1}, X_{C2}) circuit elements, however, cannot be represented by simple inductances and capacitances [7]. For the fundamental frequency band of the waveguide (no higher modes can propagate), the embedding impedance can be measured as described in [8] and [9]. In Figs. 4 and 5, measurements on some experimental mixers made using the method described in [8] are depicted. From these measurements, X_L, X_{C1}, and X_{C2} of Fig. 3 can be determined.

It is interesting to see how shortening the whisker not only moves the impedance circle downwards in the impedance diagram (corresponding to smaller inductance X_0 and X_L), but also makes the diameter of the impedance circle smaller (corresponding to a decrease in X_{C1}). In Fig. 5, the effect of going from an ordinary reduced-height waveguide to a ridged waveguide by making grooves is illustrated (Fig. 5(a) and (b)). The decrease in the waveguide impedance is observed as a decrease in the impedance circle diameter. By further decreasing the whisker length, the position of the circle moves, corresponding to a lower inductance X_L.

Short enough whisker wires (Figs. 4 and 5(c)) will leave impedance circles with diameters close to the impedance of the waveguide, indicating that X_{C1} is large compared to X_L. Similar observations have been made by Pospieszalski and Weinreb [9], [10].

0018-9480/83/0200-0230$01.00 ©1983 IEEE